

## Growth of multilayers of $\text{Bi}_2\text{Se}_3/\text{ZnSe}$ : Heteroepitaxial interface formation and strain

H. D. Li,<sup>1,2</sup> Z. Y. Wang,<sup>1</sup> X. Guo,<sup>1</sup> Tai Lun Wong,<sup>3</sup> Ning Wang,<sup>3</sup> and M. H. Xie<sup>1,a)</sup>

<sup>1</sup>Department of Physics, The University of Hong Kong, Pokfulam Road, Hong Kong

<sup>2</sup>Department of Physics, Beijing Jiaotong University, Beijing 100044, People's Republic of China

<sup>3</sup>Department of Physics, Hong Kong University of Science and Technology, Kowloon, Hong Kong

(Received 1 December 2010; accepted 4 January 2011; published online 26 January 2011)

Multilayers of  $\text{Bi}_2\text{Se}_3/\text{ZnSe}$  with the periodicity of a few nanometers were grown by molecular-beam epitaxy on Si(111). While epitaxial growth of  $\text{Bi}_2\text{Se}_3$  on ZnSe proceeded by two-dimensional nucleation, ZnSe growth on  $\text{Bi}_2\text{Se}_3$  showed the three-dimensional growth front. Therefore, the two complementary interfaces of  $\text{Bi}_2\text{Se}_3/\text{ZnSe}$  were asymmetric in morphological properties. Strain-relaxation rates were found to differ between epitaxial ZnSe and  $\text{Bi}_2\text{Se}_3$ , which could be attributed to the specific growth modes and the properties of  $\text{Bi}_2\text{Se}_3$  and ZnSe surfaces.

© 2011 American Institute of Physics. [doi:10.1063/1.3548865]

Soon after the revelation of  $\text{Bi}_2\text{Se}_3$  to be a nontrivial three-dimensional (3D) topological insulator (TI),<sup>1</sup> research of this compound has become very active. Apart from bulk crystals, nanostructured  $\text{Bi}_2\text{Se}_3$  have been fabricated for enhanced surface contributions due to increased surface-to-volume ratio.<sup>2</sup> This trend of research is encouraged further by a recent experimental finding that ultrathin  $\text{Bi}_2\text{Se}_3$  layers could be TI with tunable coupling of the surface states.<sup>3</sup>

$\text{Bi}_2\text{Se}_3$ -based superlattices or multiple quantum well/dots can be appealing for device applications. Yet, they contain multiple “surfaces” at the boundaries between TI and normal insulator “spacers,”<sup>4</sup> and thus properties related to the TI states of the matter are expectedly enhanced. In the past, superlattices of bismuth chalcogenides, particularly that of  $\text{Bi}_2\text{Te}_3/\text{Sb}_2\text{Te}_3$ , have been studied for the purpose of improving thermoelectric figure-of-merit.<sup>5,6</sup> However, reports of  $\text{Bi}_2\text{Se}_3$ -based multilayers or superlattices remain scarce. For the purpose of exploring the TI states, we seek to combine  $\text{Bi}_2\text{Se}_3$  with conventional band insulators in the form of superlattices. Among the various conventional band insulators, selenide compounds will obviously be most appropriate in view of the chemical similarity and the convenience in growth by molecular-beam epitaxy (MBE). Among the selenide compounds, ZnSe came to our attention due to its relatively large band gap ( $\sim 2.7$  eV), small lattice mismatch with  $\text{Bi}_2\text{Se}_3$  ( $\sim 3.2\%$ ), and more importantly its compatible growth conditions with that of  $\text{Bi}_2\text{Se}_3$ . Severe interface reaction between ZnSe and  $\text{Bi}_2\text{Se}_3$  can also be excluded, as only  $\sim 6$  mol % of ZnSe is soluble in  $\text{Bi}_2\text{Se}_3$  at 973 K.<sup>7</sup>

To necessitate the superlattice growth, heteroepitaxial growth behavior of ZnSe on  $\text{Bi}_2\text{Se}_3$  and  $\text{Bi}_2\text{Se}_3$  on ZnSe and their interface characteristics are first followed by reflection high-energy electron diffraction (RHEED), scanning electron microscopy (SEM), x-ray diffraction (XRD), and transmission electron microscopy (TEM). It is found that despite the differences in bonding characteristics between ZnSe (covalent) and  $\text{Bi}_2\text{Se}_3$  [covalent within the quintuple layer (QL) but van der Waals between QLs], good epitaxy of  $\text{Bi}_2\text{Se}_3$  on ZnSe with smooth surface morphology was readily achieved.

On the other hand, ZnSe growth on  $\text{Bi}_2\text{Se}_3$  showed a rough growth front. Such an asymmetry of growth behavior was accompanied by an asymmetric strain-relaxation process. Thus, the two complementary heterointerfaces, i.e., one formed by growing  $\text{Bi}_2\text{Se}_3$  on ZnSe and the other by depositing ZnSe on  $\text{Bi}_2\text{Se}_3$ , showed different morphological and structural properties.

The growth experiments were conducted in a customized MBE reactor, where source fluxes were provided from conventional Knudsen cells.<sup>8</sup> Si(111) substrate was thermally treated for the  $(7 \times 7)$  reconstruction, after which a  $\sim 200$  nm thick  $\text{Bi}_2\text{Se}_3$  buffer layer was grown following the two-step procedure as detailed in Ref. 8. Subsequent depositions of multilayers of ZnSe and  $\text{Bi}_2\text{Se}_3$  were carried out on such buffer films in the Se-rich environment (the flux ratio of Se:Bi(Zn)  $\sim 10:1$ ) and the substrate temperature was in the range of 200–300 °C. Typical growth rates were  $\sim 3$  QLs/min for  $\text{Bi}_2\text{Se}_3$  and 4 bilayers (BLs)/min ( $\sim 2$  nm/min) for ZnSe.

The surface of the  $\text{Bi}_2\text{Se}_3$  buffer film showed the typical terrace-and-step morphology, and the RHEED patterns taken from such a surface [Figs. 1(a) and 1a'] are characterized by sharp diffraction streaks aligned into the Ewald arc on screen, implying a very smooth surface of the film.<sup>8</sup> Upon initiation of ZnSe deposition at 200 °C on such a surface, we observe the RHEED pattern to change abruptly from that of  $\text{Bi}_2\text{Se}_3$  to one characteristic of a zinc-blende (zb) ZnSe [Fig. 1(b) and 1b']. This is seen by in-plane lattice parameter measurement by the RHEED [i.e., the value  $D$  as defined in Fig. 1(a)] as well as by the symmetry of the transmission diffraction spots shown in Fig. 1(c). It suggests an incommensurate lattice of epitaxial ZnSe with respect to  $\text{Bi}_2\text{Se}_3$ , reflecting the weak chemical bonding of the covalent ZnSe on a van der Waals surface of  $\text{Bi}_2\text{Se}_3$ . Similar incommensurate epitaxial relation was noted previously in systems of ZnSe-on-GaSe and -InSe, which are layered compounds with similar weak van der Waals bonding along the  $c$ -direction.<sup>9,10</sup> Thus it is likely that the weak chemical bonding at ZnSe/ $\text{Bi}_2\text{Se}_3$  interface is responsible for the incommensurate growth of ZnSe and the 3D growth mode as manifested by a quick evolution of the streaky RHEED patterns of the starting surface into a spotty one shown in Fig. 1(c). We note also, however, that in

<sup>a)</sup>Author to whom correspondence should be addressed. Electronic mail: mhxie@hku.hk.

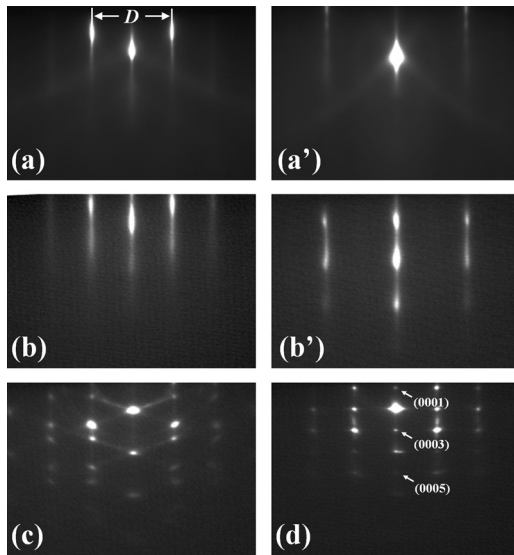


FIG. 1. RHEED patterns from a 200 nm thick  $\text{Bi}_2\text{Se}_3$  buffer film surface grown on Si(111) taken along (a) the  $[100]$  and (a')  $[210]$  azimuth directions, respectively. (b) and (b') are RHEED patterns taken from a 10 nm thick zb-ZnSe layer surface grown at 200 °C on  $\text{Bi}_2\text{Se}_3$ . (c) and (d) are RHEED patterns taken along  $[100]$  from a 30 nm thick zb-ZnSe layer grown at 200 °C on  $\text{Bi}_2\text{Se}_3$  and a 30 nm thick wz-ZnSe layer grown at 300 °C on  $\text{Bi}_2\text{Se}_3$ , respectively. In (d), the forbidden  $(000l)$  ( $l=1,3,5,\dots$ ) diffractions from wz-ZnSe are indicated by arrows.

some cases of covalent compound growth on layered substrates, such as GaAs on GaSe, smooth growth fronts were observed.<sup>11</sup> So the rough growth front of ZnSe on  $\text{Bi}_2\text{Se}_3$  may also be related to the specific chemical environment of the system.

From the symmetry of the transmission spots in Fig. 1(c), one infers the film is of a twinned zb-phase ZnSe. Increasing the growth temperature does not seem to improve the morphology of the growing surface, but affects the structural phase of the grown layer. At temperatures about 270 °C, wurtzite (wz) phase ZnSe becomes dominant as inferred also from the symmetry of the spotty RHEED patterns [Fig. 1(d)]. From Fig. 1(d), we note further that the otherwise forbidden  $(000l)$  ( $l=1,3,6,\dots$ ) diffractions of wz-ZnSe have become allowed, possibly due to multiscattering or Umweganregung effect.<sup>12</sup> Experiments at temperatures higher than 300 °C was not attempted here due to a possible phase transition and dissociation of  $\text{Bi}_2\text{Se}_3$ .

Growth of  $\text{Bi}_2\text{Se}_3$  on ZnSe, not surprisingly, proceeds by a two-dimensional (2D) mode. In fact, we find that the growing  $\text{Bi}_2\text{Se}_3$  tends to smooth a relatively rough ZnSe surface underneath. The slight spotty RHEED patterns of a starting ZnSe surface recovers to a streaky one after a thickness of  $\text{Bi}_2\text{Se}_3$  deposition. In Fig. 2(a), we present a high-resolution transmission electron microscopy (HRTEM) micrograph showing the interface of  $\text{Bi}_2\text{Se}_3$ -on-ZnSe. The sample consists of a  $\sim 10$  nm thick  $\text{Bi}_2\text{Se}_3$  layer deposited on a 20 nm thick ZnSe film. The latter itself is grown on a  $\text{Bi}_2\text{Se}_3/\text{Si}(111)$  substrate. Note that the surface of the ZnSe layer is already roughened and the layer is of single domain zb-phase according to the TEM and transmission electron diffraction (TED) examinations [Fig. 2(c)]. The grown  $\text{Bi}_2\text{Se}_3$  on ZnSe is of the rhombohedral structure consisting of -Se-Bi-Se-Bi-Se- QL units in the  $[001]$  direction. A zoom-in image of the HRTEM [Fig. 2(b)] reveals the atomic registry of  $\text{Bi}_2\text{Se}_3/\text{ZnSe}$  interface. A lattice coherency may

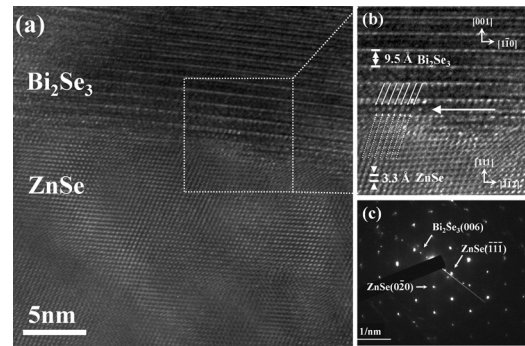


FIG. 2. (a) HRTEM image taken along the  $[\bar{1}10]_{\text{ZnSe}}$  zone axis of a sample containing heteroepitaxial layers of  $\text{Bi}_2\text{Se}_3$  and ZnSe. (b) A zoom-in image of (a) in the region labeled. (c) TED image of the sample.

be found. The RHEED measurements of in-plane lattice parameter reveal a gradual relaxation from that of ZnSe to  $\text{Bi}_2\text{Se}_3$ , contrasting to the abrupt relaxation for ZnSe deposition on  $\text{Bi}_2\text{Se}_3$ . This is further demonstrated in Fig. 4(a), a recorded lattice profile during multiple layers growth. A careful examination of the atomic alignment of  $\text{Bi}_2\text{Se}_3$  and ZnSe [refer to the dashed and solid arrow arrays in Fig. 2(b)] reveals an atomic stacking sequence of the epitaxial  $\text{Bi}_2\text{Se}_3$  to inherit that of the underlying zb-ZnSe in the reversing order, i.e., from ...ABCA... of ZnSe to ...CBAC... of  $\text{Bi}_2\text{Se}_3$ , along the growth direction. The epitaxial relationship between  $\text{Bi}_2\text{Se}_3$  and ZnSe at the interface can thus be inferred to as  $\text{Si}(111)[\bar{1}\bar{1}2] \parallel \text{Bi}_2\text{Se}_3(001)[1\bar{1}0]$ .

The morphological difference of the surfaces of ZnSe-on- $\text{Bi}_2\text{Se}_3$  and that of  $\text{Bi}_2\text{Se}_3$ -on-ZnSe can be further unveiled from SEM images shown in Fig. 3. A 30 nm thick ZnSe film grown on  $\text{Bi}_2\text{Se}_3$  at 200 °C [Figs. 3(a) and 3(b)] shows a surface containing oppositely oriented triangular islands or grains with lateral sizes smaller than 100 nm and some tall but faceted 3D islands of sizes of  $\sim 50$  nm. This is consistent with the spotty RHEED patterns from such surfaces. On the other hand, for a film of  $\text{Bi}_2\text{Se}_3$  grown on ZnSe at similar thicknesses, much smoother morphologies can be observed as exemplified in Figs. 3(c) and 3(d). This is despite that the underlying ZnSe film surface is slightly rough. From Figs. 3(c) and 3(d), we may still note the existence of

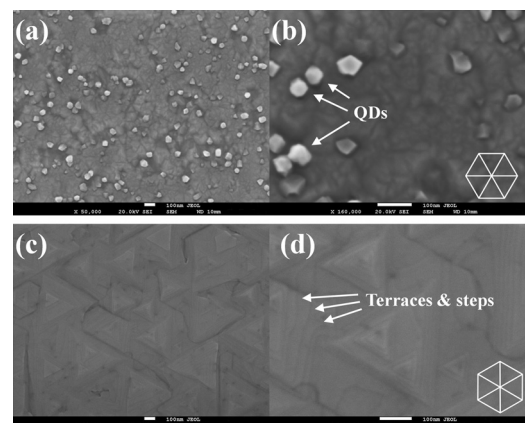


FIG. 3. High resolution SEM images of surfaces of [(a) and (b)] 30 nm thick ZnSe grown on  $\text{Bi}_2\text{Se}_3$  and [(c) and (d)] 20 nm thick  $\text{Bi}_2\text{Se}_3$  on ZnSe. The magnifications in (a), (b), (c), and (d) are 50 000, 160 000, 50 000, and 150 000, respectively. The crystallographic directions of the films are indicated by white hexagons drawn.

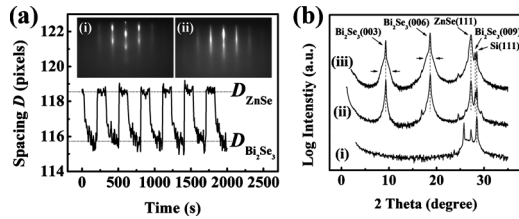


FIG. 4. (a) Reciprocal lattice parameter evolution during growth of a multilayer structure and the insets show the RHEED patterns of the last (i) ZnSe and (ii) Bi<sub>2</sub>Se<sub>3</sub> layers of the structure. (b) XRD  $\theta$ - $2\theta$  scans from (i) Si(111) substrate, (ii) 10-periods, and (iii) 20-periods of ZnSe/Bi<sub>2</sub>Se<sub>3</sub>, respectively.

twinned grains (manifested by the oppositely oriented triangles), the sizes of which are of the order of  $\sim 300$  nm, significantly larger than those in ZnSe. Notably, there is no tall 3D island on the surface of Bi<sub>2</sub>Se<sub>3</sub>, agreeing again with the RHEED observation that Bi<sub>2</sub>Se<sub>3</sub> growth on ZnSe proceeds via 2D nucleation.

The (reciprocal) lattice parameter evolution during growth of a superlattice of ...ZnSe/Bi<sub>2</sub>Se<sub>3</sub>/ZnSe... is measured in real time by RHEED, and the result is presented in Fig. 4(a). The thickness of ZnSe and Bi<sub>2</sub>Se<sub>3</sub> layers are 6 and 9 nm, respectively. As is seen, the in-plane lattice constant of epitaxial ZnSe takes its theoretical (strain-free) value abruptly whereas that of Bi<sub>2</sub>Se<sub>3</sub> on ZnSe relaxes more gradually. This is associated with the 3D and 2D growth modes of the two cases and the corresponding RHEED patterns taken at the last round of the 20-period growth are shown in the inset of Fig. 4(a). Such a strain-relaxation behavior is not so unexpected, as after all a relatively inert surface of Bi<sub>2</sub>Se<sub>3</sub> will not provide much constraint to the lattices of epitaxial ZnSe. Added by the 3D growth front, atoms are more relaxed so as to take the equilibrium positions. On the other hand, for 2D growth of Bi<sub>2</sub>Se<sub>3</sub> on the covalent ZnSe compound surface, atoms of the deposit likely form chemical bonds with those of the substrate. The 2D growth front of Bi<sub>2</sub>Se<sub>3</sub> makes lattice strain relaxation less easily but via line and/or plane defects at the interfaces. Another point of relevance is that for ZnSe growth on Bi<sub>2</sub>Se<sub>3</sub>, the strain is tensile, which is known to be less easily accommodated by elastic deformation of the lattices than a compressively strained case.<sup>13</sup> XRD measurements of the grown superlattice samples are shown in Fig. 4(b), where curves (i)–(iii) represent the  $\theta$ - $2\theta$  scans of Si (the substrate), 10-periods, and 20-periods of ZnSe/Bi<sub>2</sub>Se<sub>3</sub> on Si(111), respectively. Peaks at the  $2\theta$  angles of 9.32°, 18.64°, and 28.1° are from Bi<sub>2</sub>Se<sub>3</sub> [correspond to (003), (006), and (009) diffractions], while those at 27.24° and 28.46° are of ZnSe(111) and Si(111), respectively. The very weak peaks at 29.44° may be associated with Bi<sub>2</sub>Se<sub>3</sub>(015) due to tilting of the film but the others may be attributed to the nonmonochromaticity of the x-ray or to Si substrate [cf. Fig. 4(b)(i)]. We observe no satellite peak, probably due to nonideal heterointerfaces and/or nonuniformity of the layer thickness. As is evident by comparing the

10-period to the 20-period sample [i.e., curves (ii) and (iii)], increasing the total thickness of the multilayers causes more broadened tails of the diffraction peaks. This is related to the decreasing quality of the grown layers as well as to the accumulation of residual strains at different Bi<sub>2</sub>Se<sub>3</sub>/ZnSe interfaces.

To summarize, epitaxial growth of ZnSe on Bi<sub>2</sub>Se<sub>3</sub> and Bi<sub>2</sub>Se<sub>3</sub> on ZnSe have been studied, where the 3D and 2D growth fronts are observed for the two complementary cases. Strain relaxation show slightly different behaviors that are connected to the different characteristics of the surfaces and growth modes. Multiple layers consisting of alternating ZnSe and Bi<sub>2</sub>Se<sub>3</sub> epilayers have been grown. However, due to non-ideal heterointerfaces and structural uniformity, satellite peaks are not detected by the XRD measurements. It is important therefore to improve the quality of the heterointerfaces, especially that of Bi<sub>2</sub>Se<sub>3</sub>-on-ZnSe, which is inherently rough due to the rough growth front of ZnSe-on-Bi<sub>2</sub>Se<sub>3</sub>. Alternatively, other spacing layers than ZnSe may be sought for growing Bi<sub>2</sub>Se<sub>3</sub>-based superlattice or multiple quantum well structures.

The authors wish to acknowledge the technical support from W.K. Ho and S.Y. Chui in the growth and XRD experiments, respectively. The project is financially supported by a General Research Fund (Grant No. HKU 7061/10P) and a Collaborative Research Fund (Grant No. HKU 10/CRF/08) from the Research Grant Council of Hong Kong Special Administrative Region (HKSAR), as well as a Seed Fund for Basic Research from HKU.

- <sup>1</sup>H. J. Zhang, C. X. Liu, X. L. Qi, X. Dai, Z. Fang, and S. C. Zhang, *Nat. Phys.* **5**, 438 (2009); Y. Xia, D. Qian, D. Hsieh, L. Wray, A. Pal, H. Lin, A. Basil, D. Grauer, Y. S. Hor, R. J. Cava, and M. Z. Hasan, *ibid.* **5**, 398 (2009).
- <sup>2</sup>H. Peng, K. Lai, D. Kong, S. Meister, Y. Chen, X.-L. Qi, S.-C. Zhang, Z.-X. Shen, and Y. Cui, *Nature Mater.* **9**, 225 (2010); S. S. Hong, W. Kundhikanjana, J. J. Cha, K. J. Lai, D. S. Kong, S. Meister, M. A. Kelly, Z. X. Shen, and Y. Cui, *Nano Lett.* **10**, 3118 (2010).
- <sup>3</sup>Y. Zhang, K. He, C. Z. Chang, C. L. Song, L. L. Wang, X. Chen, J. F. Jia, Z. Fang, X. Dai, W. Y. Shan, S. Q. Shen, Q. Niu, X. L. Qi, S. C. Zhang, X. C. Ma, and Q. K. Xue, *Nat. Phys.* **6**, 584 (2010).
- <sup>4</sup>J. H. Song, H. Jin, and A. J. Freeman, *Phys. Rev. Lett.* **105**, 096403 (2010).
- <sup>5</sup>R. Venkatasubramanian, E. Siivola, T. Colpitts, and B. O'Quinn, *Nature (London)* **413**, 597 (2001).
- <sup>6</sup>M. S. Dresselhaus, G. Chen, M. Y. Tang, R. G. Yang, H. Lee, D. Z. Wang, Z. F. Ren, J. P. Fleurial, and P. Gogna, *Adv. Mater.* **19**, 1043 (2007).
- <sup>7</sup>V. V. Marugin, I. N. Odin, and A. V. Novoselova, *Zh. Neorg. Khim.* **28**, 2104 (1983).
- <sup>8</sup>H. D. Li, Z. Y. Wang, X. Kan, X. Guo, H. T. He, Z. Wang, J. N. Wang, T. L. Wang, N. Wang, and M. H. Xie, *New J. Phys.* **12**, 103038 (2010).
- <sup>9</sup>E. Wisotzki, A. Klein, and W. Jaegermann, *Thin Solid Films* **380**, 263 (2000).
- <sup>10</sup>E. Wisotzki, A. Klein, and W. Jaegermann, *Adv. Mater.* **17**, 1173 (2005).
- <sup>11</sup>J. E. Palmer, T. Saitoh, T. Yodo, and M. Tamura, *J. Appl. Phys.* **74**, 7211 (1993); *J. Cryst. Growth* **150**, 685 (1995).
- <sup>12</sup>J. Bläsing and A. Krost, *Phys. Status Solidi A* **201**, R17 (2004).
- <sup>13</sup>J. E. Prieto and I. Markov, *Phys. Rev. B* **72**, 205412 (2005).